Electronic Structure of DNA Nucleobases and Their Dinucleotides Explored by Soft X-ray Spectroscopy

Yoshihisa Harada,*,† Tomoyuki Takeuchi,† Hiori Kino,‡ Akiko Fukushima,§ Kaoru Takakura,|| Kotaro Hieda,⊥ Aiko Nakao,# Shik Shin,†,@ and Hidetoshi Fukuyama¥

Riken SPring-8 Center, 1-1-1 Kouto Sayo-cho Sayo-gun Hyogo 679-5148, Japan, National Institute for Materials Science, 1-2-1 Sengen Tsukuba Ibaraki 305-0047, Japan Photon Factory, Institute of Materials Structure Science, High Energy Accelerator Research Organization, 1-1 oho Tsukuba Ibaraki 305-0801, Japan, Division of Natural Sciences, International Christian University, 3-10-2 Osawa Mitaka Tokyo Department of Chemistry, College of Science, Rikkyo University, 3-34-1 Nishi-Ikebukuro Toshimaku Tokyo 171-8501, Japan, The Institute of Physical and Chemical Research, 2-1 Hirosawa Wako Saitama 351-0198, Japan, Institute for Solid State Physics, University of Tokyo, 5-1-5 Kashiwanoha Kashiwa Chiba 277-8581, Japan, and International Frontier Center for Advanced Materials, Institute for Materials Research, Tohoku University, 2-1-1 Katahira Aoba-ku Sendai Miyagi 980-8577, Japan

Received: May 3, 2006; In Final Form: September 4, 2006

The electronic structures of a series of DNA nucleobases and their dinucleotides were investigated by N 1s X-ray absorption, X-ray photoemission, and resonant X-ray emission spectroscopy. Resonant X-ray emission spectra of the guanine base and its dinucleotide indicate that it has a weak structure at the lowest binding energy; at this energy, it isolates from the main valence band and forms the HOMO state. This indicates that the HOMO state is localized in the guanine base, as claimed by valence and core photoemissions and expected from theoretical predictions. In addition, the XAS and XES profiles of the guanine dinucleotide indicate that disruption of the aromatic character of the six-membered ring results in the localization of the π state at the imine (−N═) site of the guanine base; this may favor charge transfer among stacked guanine bases and further influence the conductivity of DNA.

Introduction

Since the early 1960s, a decade after the discovery of the double helix structure of DNA by Watson and Crick,[1] there have been numerous experimental reports on the transport properties of DNA.[2−10] The chemistry of DNA fibers can be controlled and tuned by acting on the sequential combination of its four nucleobases, thymine, adenine, guanine, and cytosine. Several contradictory experimental results have been reported, wherein DNA has been claimed to be a wide gap semiconductor[6] to a metal,[4] and even a superconductor.[9] This clearly indicates that these experiments are very delicate to perform, since they involve the handling of single DNA double-strands and their interaction with a support having metallic contacts.[11] Recently, some ambiguities related to the differences in the experimental results appear to have been resolved.[12−15] Kino et al. suggested that the electronic states of an anhydrous cation can form a lowest unoccupied molecular orbital (LUMO) very close to the valence band and can dope a hole into the highest occupied molecular orbital (HOMO) localized in the stacked base pairs; this could be one of the possible reasons for the conductivity of DNA.[14] This implies that just as the conductivity of ordinary semiconductors can be controlled by carrier doping, the conductivity of DNA can be controlled by changing the amount of holes doped by anhydrous cations.

In order to understand the underlying principles leading to the above scenario, it is important to know the electronic states of DNA near the band gap. These states are, in each case, determined by a combination of electronic states, which are derived from the nucleobases, ribose rings, phosphates, and counter ions. Further, they are affected by the C−N glycosidic bond between the anomeric carbon of the ribose and the nitrogen of a nucleobase, hydrogen bonds between a base pair, and stacking of the nucleobases. In order to disentangle all these concurrent effects and learn more about the DNA HOMO−LUMO states, we need to study the valence electronic structures of the building blocks of DNA, i.e., the single nucleobases and nucleotides.

Very recently, MacNaughton et al. reported the electronic structure of the nucleobases; unoccupied and occupied electronic structures were elucidated using soft X-ray absorption spectroscopy (XAS) and X-ray emission spectroscopy (XES).[16] Figure 1 illustrates the transitions involved in XAS and XES. XES is known to be a bulk-sensitive method since it involves the photon-in and photon-out processes.[17−19] XES is also applicable to wet materials.[20] Although photoemission spectroscopy (PES) of DNA provides the global density of states (DOS) relevant to the valence electrons,[21] XES is advantageous since it provides element specificity and allows symmetry selection, which provides the partial DOS of a particular element.[17−19]

In this paper, we discuss the electronic structure of the nucleobases and their dinucleotides. We measured N 1s XAS, X-ray photoemission spectroscopy (XPS), and XES. Since the

* To whom correspondence should be addressed. E-mail: harada@spring8.or.jp.
† Riken SPring-8 Center.
‡ National Institute for Materials Science.
§ Photon Factory.
|| International Christian University.
⊥ Rikkyo University.
The Institute of Physical and Chemical Research.
@ University of Tokyo.
¥ Tohoku University.

10.1021/jp062720j CCC: $33.50
Published on Web 11/18/2006

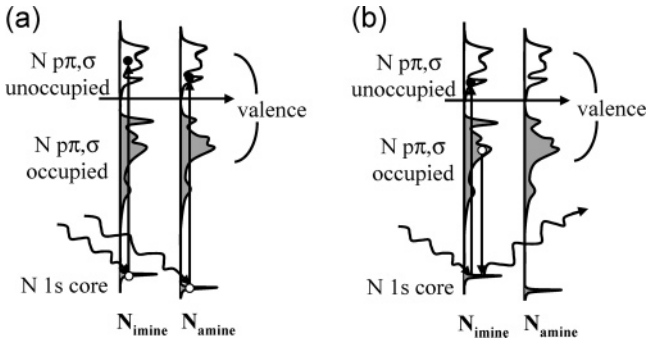

Figure 1. Schematic drawing of (a) N 1s XAS and (b) N 1s XES. Tuning the excitation energy to the lowest π^* peak, we obtain the partial occupied DOS at the imine site by N 1s XES.

nitrogen atom is only included in the nucleobases, N 1s core excitation was used to observe the changes in the electronic structure of the nucleobases, which will provide complementary information to C 1s or O 1s core spectroscopy that is also essential to unravel the electronic structure of nucleobases, nucleotides, or amino acids.[16,22−24] More specifically, the nucleobases show the presence of two characteristic nitrogen sites, i.e., imine (−N═) and amine (−N−) sites, which have different core levels due to chemical shift. In order to elucidate site-specific information, we used resonant XES by tuning the excitation energy so that it was sensitive to particular sites.[25] The resonant XES in Figure 1 illustrates a particular case, selecting the imine site. These results were compared to those obtained by PES[21] and resonant Auger electron spectroscopy,[26] thus it was demonstrated that unique information can be obtained using resonant XES.

Materials and Methods

A single crystal of a series of nucleobases, i.e., adenine, guanine, cytosine, and thymine, was prepared by one of us (K.T.), and their dinucleotide powders were purchased from Hokkaido System Science Co. Ltd. The dinucleotide powders were solvated in distilled water to yield a concentration of 5 mg/mL; 150 μL of the solvated sample was dropped on a copper sample plate and dried overnight in a desiccator. No further purification was carried out.

N 1s XAS and XES measurements were performed at BL-19B[27] and BL-2C,[28] respectively, at Photon Factory, KEK. The XAS spectra were obtained at BL-19B by measuring the total X-ray fluorescence using a Si photodiode, and the XES spectra were obtained at BL-2C using a Rowland mount type soft X-ray emission spectrometer with a holographic grating of 5 m radius and 1200 lines/mm.[29]

The total energy resolution of the XAS and XES spectra was 0.1 and 0.5 eV, respectively. The incidence angle of the excitation beam to the sample normal was fixed to 70°. The samples were cooled to 40 K and the sample position was changed every 5 min to minimize the radiation damage caused by intense X-rays at 10^{13} photons/(s•cm^2).

In order to plot the XES spectra against binding energy, we also measured the N 1s XPS of the four nucleobases and their dinucleotides. XPS measurements were carried out using a VG ESCALAB 250 spectrometer (Thermo Electron Co.) that employed monochromatic X-ray AlK (1486.6 eV, 200 W) radiation. In order to avoid any charge build-up, the samples were masked using a copper tape with a nonfocused 4 eV electron shower. Overcompensation was tuned by taking the binding energy of the C−C bonding to be 285.0 eV.[30] The obtained spectra were decomposed into a relevant number of Gaussian peaks, and the binding energy of the lowest component was used to plot the XES spectra against binding energy.

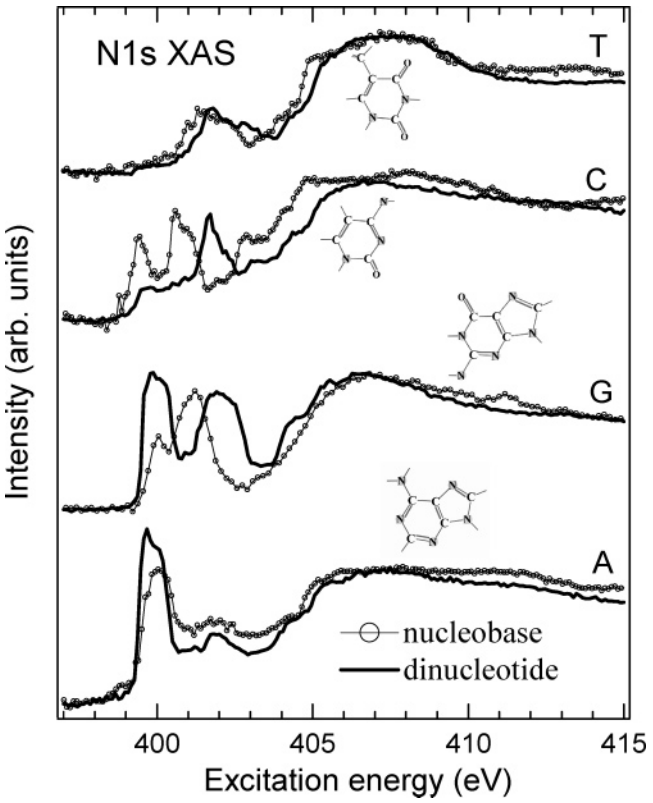

Figure 2. N 1s XAS spectra of adenine, guanine, cytosine, thymine, and their dinucleotides. Schematic diagrams of the four nucleobases are also shown beside the spectra.

From the XPS measurements, we confirmed that the dinucleotides did not include sodium ions as counter cations attached to the outermost phosphate group. These sodium ions may have been in the form of anhydrous cations under high vacuum and played a role in the transport properties.[14] Thus, the differences between the nucleobases and their dinucleotides discussed in this paper may be due to the C−N glycosidic bond as well as the outermost phosphate.

We also calculated N 2p partial DOS at a specific nitrogen site for nucleobases. The Gaussian03 package[31] was used for the density functional theory with the gradient corrected correlation functional (PW91). The 6-31G(d,p) basis set was employed to relax atomic positions. The 6-311+G(3df, 3pd) basis set was used to calculate eigenenergies. The N 2p partial DOS of a specific nitrogen site having the lowest N 1s binding energy was compared with the experimental results, whereas those of other nitrogen sites were also taken in the spectra by exponential decay $\exp(-\Delta\Omega\tau_c/h)$, where $\Delta\Omega$ indicates an energy detuned from the resonance calculated by difference in the N 1s binding energy, τ_c is the lifetime of the N 1s core hole, and h is the Planck constant. We applied $\tau_c = 4.7$ fs for this study.[32]

Results and Discussion

Figure 2 shows the N 1s XAS spectra of the four nucleobases and their dinucleotides. The molecular structure of each nucleobase is sketched beside its spectrum. The profile of the XAS spectra can be separated into two π^* states below 403 eV, σ^* states around 405 eV and a resonance state beyond these energy levels.[33,34] The lower and higher π^* peaks primarily correspond to the imine and amine sites, respectively. The π^* states at the

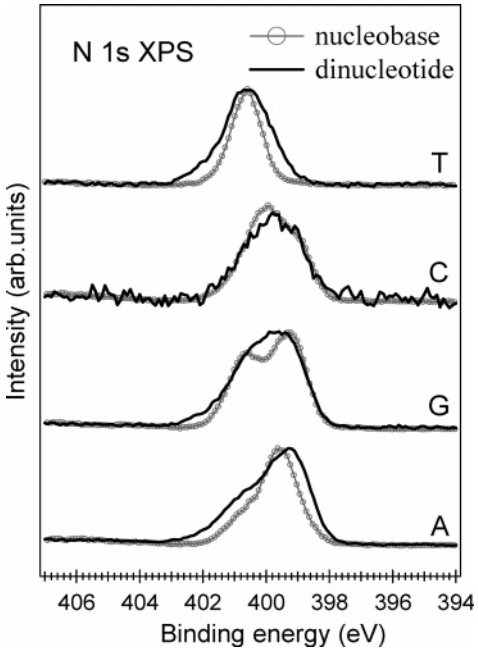

Figure 3. N 1s XPS spectra of the four nucleobases and their dinucleotides.

amine sites of guanine and cytosine are shifted toward a higher energy level for the corresponding dinucleotides. According to Kirtley et al., the aromatic character of the six-membered ring of guanine and cytosine may be disrupted by the C−N glycosidic bond,[33] which results in a blue shift of the π^* state at the amine sites. It is possible that the amine site in the six-membered ring is responsible for the shift to a higher π^* peak since a six-membered ring with both imine and amine sites is exclusive to guanine and cytosine. However, as shown in Figure 3, the shift is not clearly recognized in the N 1s XPS spectra of their dinucleotides. Thus, the peak shift in the XAS spectra of guanine and cytosine dinucleotides may be mainly due to a change in the valence electronic structure, rather than due to a chemical shift.

Figure 4 shows the N 1s XES spectra of the nucleobases obtained by resonant excitation to the π^* states at the imine sites. They are plotted as a function of binding energy. For thymine, we used the XES spectra that were obtained by excitation below the absorption edge by ΔE and plotted it as a function of the energy difference (binding energy $-\Delta E$). This procedure is crucial when plotting an XES spectrum as a function of binding energy while assuming that the XES spectrum shifts linearly until the excitation energy reaches the absorption edge. Generally, features above 8 eV correspond to the emission from σ orbitals, whereas those below 8 eV correspond to the emission from π orbitals. Since we used the lowest π^* peak as the excitation energy, the XES spectrum reflects the DOS at the imine sites. Crosses on the cytosine spectrum indicate false structures that were produced by X-ray irradiation-induced damage. Figure 4 also shows the calculated N 2p partial DOS spectra of the nucleobases at the imine sites, which have been shifted 0.6 eV toward the lower binding energy in order to align the overall profile with the experimental result. Electronic structures from σ and π contributions are displayed separately. The calculation is approximately consistent with the experiment apart from the intensity at higher binding energy in thymine and at lower binding energy in adenine. An isolated structure appears around 4 eV on the guanine XES spectrum in Figure 4. Compared with the calculation, this can be assigned as the π state at the imine site that forms the HOMO level. Further, the HOMO level of guanine is slightly higher than that of other nucleobases. This is in agreement with the results of previous works in that guanine contributes to the HOMO state in DNA.[35]

Figure 5 compares the N 1s XES spectra of guanine and its dinucleotide; the spectra were obtained by resonant excitation to the π^* states at the imine sites. The valence emission spectra at the imine sites of both guanine and its dinucleotide indicate

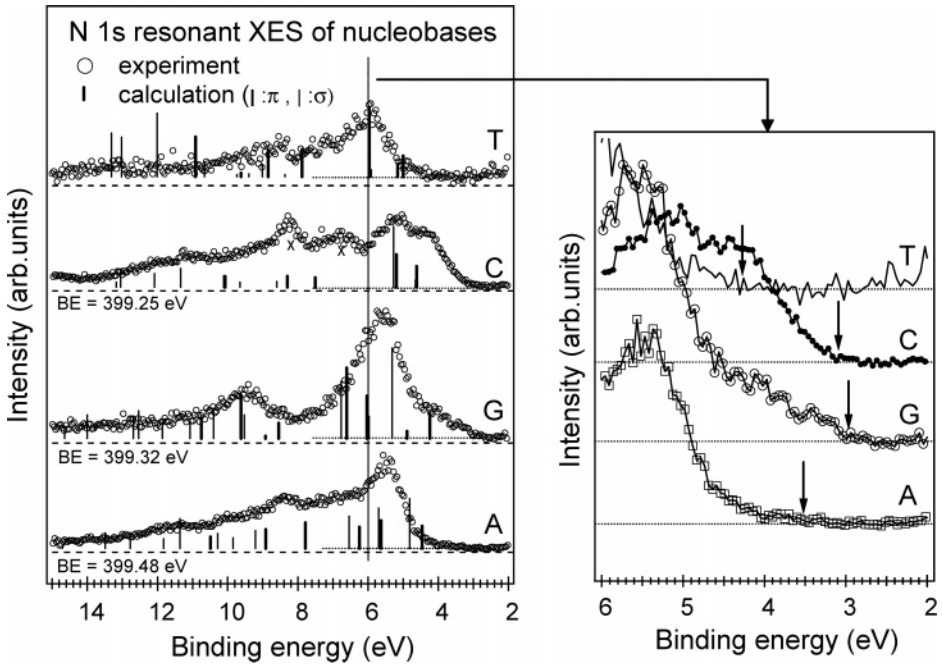

Figure 4. N 1s XES spectra of the nucleobases observed by resonant excitation of the imine (−N═) site (left panel) and enlarged spectra near the valence band top (right panel). They are plotted against binding energy by using the N 1s core levels measured by XPS, which are described below each spectrum. The horizontal dotted lines and vertical arrows (right panel) act as guides to identify the HOMO level of each nucleobase. The horizontal dashed lines indicate the baseline of the detector to indicate the offset level of the signal. Further, the calculated DOSs around the excited atom are shown as line spectra. Crosses on the cytosine spectrum indicate false structures that were produced by X-ray irradiation-induced damage.

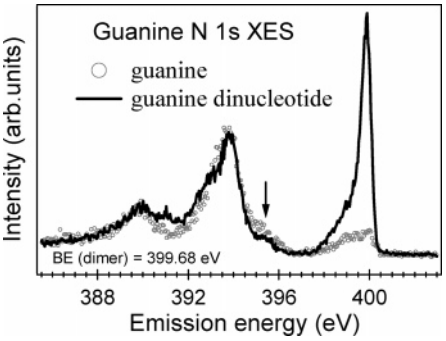

Figure 5. N 1s XES spectra of guanine and its dinucleotide observed by resonant excitation at the imine sites. The asymmetric single peak above 397 eV corresponds to the recombination emission.

isolated structures at the top of the valence band. According to Yang et al., the isolated structure is also observed in the valence PES spectra of the guanine dinucleotide.[21] By comparing DFT calculations with the PES results, Yang et al. suggested that the isolated structure that corresponds to the HOMO state is localized in the guanine base. In the XES spectra of the guanine dinucleotide, as indicated by an arrow, the highest peak loses its intensity slightly, but maintains its isolated structure. Since N 1s XES probes the electronic structures that are located on the nucleobases, the presence of the isolated structure in the XES spectrum of the guanine dinucleotide indicates that the HOMO state is fairly localized on the guanine base. XES provides further information about the localization of the HOMO state. The highest asymmetric peak above 397 eV corresponds to vibronic excitations that accompany direct recombination.[36−39] Since the local coordination around the excited atom is almost the same in guanine and its dinucleotide, the symmetry and frequencies of the local vibrations that couple to the short-lived core excited-state should be the same. Consequently, we can assume that the strength of the low-energy tail depends on the character of the excited state; in particular, it depends on the behavior of the excited electron during the lifetime of the core hole, which may be a marker for the localization of the π^* states. The argument is basically the same as that previously made by Kato et al. regarding the resonant Auger emission spectra of nucleobases in DNA duplexes.[26] Incidentally, the intensity of the elastic peaks is not necessarily a marker for the localization. One should be careful when discussing the intensity of an elastic peak, since it is easily influenced by surface conditions or other scattering factors. As shown in Figure 5, the resonant XES spectrum at the imine sites of the guanine dinucleotide has a more intense low-energy tail than that of guanine, even after taking into account the intense elastic peak. Hence, the π^* state at the imine sites of the guanine dinucleotide has a more localized character than that of guanine.

Conclusion

Combined with the XAS and XPS results, we conclude that the HOMO state of the guanine dinucleotide is localized on the guanine base. Further, we suggest that the aromatic character of the six-membered ring of the guanine dinucleotide is disrupted, which leads to an enhanced splitting of the $\pi-\pi^*$ states at the amine sites as well as an enhanced localization of the $\pi-\pi^*$ states at the imine sites in the six-membered ring. When holes are doped into the guanine base by counter cations attached to the outermost phosphate, the C−N glycosidic bond may confine the doped holes to the HOMO state by the enhanced localization of the π state at the imine site. Thus, it may play an important role in the electronic conductivity of DNA.

Acknowledgment. We would like to thank Dr. M. Furukawa for fruitful discussion. We acknowledge Prof. M. Boero for his critical reading of the manuscript. This work is partly supported by a Grant-in-Aid for Scientific Research from the Ministry of Education, Culture, Sports, Science and Technology.

References and Notes

(1) Watson, J. D.; Crick, F. H. C. *Nature* **1953**, *171*, 737.
(2) Murphy, C. J.; Arkin, M. R.; Jenkins, Y.; Ghatlia, N. D.; Bossmann, S. H.; Turro, N. J.; Barton, J. K. *Science* **1993**, *262*, 1025.
(3) Braun, E.; Eichen, Y.; Sivan, U.; Ben-Yoseph, G. *Nature* **1998**, *391*, 775.
(4) Fink, H.; Schonenberger, C. *Nature* **1999**, *398*, 407.
(5) de Pablo, P. J.; Gómez-Navarro, C.; Colchero, J.; Serena, P. A.; Gómez-Herrero, J.; Baró, A. M. *Phys. Rev. Lett.* **2000**, *85*, 4992.
(6) Porath, D.; Bezryadin, A.; De Vries, S.; Dekker, C. *Nature* **2000**, *403*, 635.
(7) Cai, L.; Tabata, H.; Kawai, T. *Appl. Phys. Lett.* **2000**, *77*, 3105.
(8) Yoo, K.-H.; Ha, D. H.; Lee, J.-O.; Park, J. W.; Kim, Jinhee; Kim, J. J.; Lee, H.-Y.; Kawai, T.; Choi, H. Y. *Phys. Rev. Lett.* **2001**, *87*, 198102.
(9) Kasumov, A. Y.; Kociak, M.; Gueron, S.; Reulet, B.; Volkov, V. T.; Klinov, D.V.; Bouchiat, H. *Science* **2001**, *291*, 280.
(10) Taniguchi, M.; Lee, H.-Y.; Tanaka, H.; Kawai T. *Jpn. J. Appl. Phys.* **2003**, *42*, L215.
(11) Gómez-Navarro, C.; Moreno-Herrero, F.; de Pablo, P. J.; Colchero, J.; Gómez Herrero, J.; Baró, A. M. *Proc. Nat. Acad. Sci. U.S.A.* **2002**, *99*, 8484.
(12) Endres, R. G.; Cox, D. L.; Singh, R. R. P. *Rev. Mod. Phys.* **2004**, *76*, 195.
(13) Gervasio, F. L.; Carloni, P.; Parrinello, M. *Phys. Rev. Lett.* **2002**, *89*, 108102.
(14) Kino, H.; Tateno, M.; Boero, M.; Torres, J. A.; Ohno, T.; Terakura, K.; Fukuyama, H. *J. Phys. Soc. Jpn.* **2004**, *73*, 2089.
(15) Gervasio, F. L.; Laio, A.; Parrinello, M.; Boero, M. *Phys. Rev. Lett.* **2005**, *94*, 158103.
(16) MacNaughton, J.; Moewes A.; Kurmaev, E. Z. *J. Phys. Chem. B* **2005**, *109*, 7749.
(17) Ederer, D. L.; Carlisle, J. A.; Jimenez. J.; Jia, J. J.; Osborn, K.; Callcott, T. A.; Perera, R. C. C.; Underwood, J. H.; Terminello, L. J.; Asfaw A.; Himpsel, F. J. *J. Vac. Sci. Technol. A* **1996**, *14*, 859.
(18) Nordgren, J.; Kurmaev, E. Z. Eds., Soft X-Ray Emission Spectroscopy, *J. Electron Spectrosc. Relat. Phenom.* **2000**, *110*−111., 1−363.
(19) Kotani, A.; Shin, S. *Rev. Mod. Phys.* **2001**, *73*, 203.
(20) Guo, J.-H.; Luo, Y.; Augustsson, A.; Rubensson, J.-E.; Sathe, C.; Agren, H.; Siegbahn, H.; Nordgren, J. *Phys. Rev. Lett.* **2002**, *89*, 137402.
(21) Yang, X.; Wang, X.-B.; Vorpagel, E.R.; Wang, L.-S. *Proc. Natl. Acad. Sci. USA* **2004**, *44*, 1197.
(22) Carravetta, V.; Plashkevych, O.; Agren, H. *J. Chem. Phys.* **1998**, *109*, 1456.
(23) Kaznacheyev, K.; Osanna, A.; Jacobsen, C.; Plashkevych, O.; Vahtras, O.; Agren, H.; Carravetta, V.; Hitchcock, A. P. *J. Phys. Chem. A* **2002**, *106*, 3153.
(24) Boese, J.; Osanna, A.; Jacobsen, C.; Kirz, J. *J. Electron Spectrosc. Relat. Phenom.* **1997**, *85*, 9.
(25) Guo, J.-H.; Butorin, S.M.; Wassdahl, N.; Skytt, P.; Nordgren, J. *Phys. Rev. B* **1994**, *49*, 1376.
(26) Kato, H. S.; Furukawa, M.; Kawai, M.; Taniguchi, M.; Kawai, T.; Hatsui, T.; Kosugi, N. *Phys. Rev. Lett.* **2004**, *93*, 086403.
(27) Fujisawa, M.; Harasawa, A.; Agui, A.; Watanabe, M.; Kakizaki, A.; Shin, S.; Ishii, T.; Kita, T.; Harada, T.; Saitoh, Y.; Suga, S. *Rev. Sci. Instrum.* **1996**, *67*, 345.
(28) Watanabe, M.; Toyoshima, A.; Azuma, Y.; Hayaishi, T.; Yan, Y.; Yagishita, A. *Proc. SPIE Int. Soc. Opt. Eng.* **1997**, *58*, 3150.
(29) Harada, Y.; Ishii, H.; Fujisawa, M.; Tezuka, Y.; Shin, S.; Watanabe, M.; Kitajima, Y.; Yagishita, A. *J. Synchrotron Radiat.* **1998**, *5*, 1013.
(30) Briggs, D.; Seah, M. P. *Practical Surface Analysis*, 2nd ed.; John Wiley and Sons Ltd.: New York, 1990; Vol. 1.
(31) Frisch, M. J.; Trucks, G. W.; Schlegel, H. B.; Scuseria, G. E.; Robb, M. A.; Cheeseman, J. R.; Montgomery, J. A., Jr.; Vreven, T.; Kudin, K. N.; Burant, J. C.; Millam, J. M.; Iyengar, S. S.; Tomasi, J.; Barone, V.; Mennucci, B.; Cossi, M.; Scalmani, G.; Rega, N.; Petersson, G. A.; Nakatsuji, H.; Hada, M.; Ehara, M.; Toyota, K.; Fukuda, R.; Hasegawa, J.; Ishida, M.; Nakajima, T.; Honda, Y.; Kitao, O.; Nakai, H.; Klene, M.; Li, X.; Knox, J. E.; Hratchian, H. P.; Cross, J. B.; Bakken, V.; Adamo, C.; Jaramillo, J.; Gomperts, R.; Stratmann, R. E.; Yazyev, O.; Austin, A. J.; Cammi, R.; Pomelli, C.; Ochterski, J. W.; Ayala, P. Y.; Morokuma, K.; Voth, G. A.; Salvador, P.; Dannenberg, J. J.; Zakrzewski, V. G.; Dapprich,

S.; Daniels, A. D.; Strain, M. C.; Farkas, O.; Malick, D. K.; Rabuck, A. D.; Raghavachari, K.; Foresman, J. B.; Ortiz, J. V.; Cui, Q.; Baboul, A. G.; Clifford, S.; Cioslowski, J.; Stefanov, B. B.; Liu, G.; Liashenko, A.; Piskorz, P.; Komaromi, I.; Martin, R. L.; Fox, D. J.; Keith, T.; Al-Laham, M. A.; Peng, C. Y.; Nanayakkara, A.; Challacombe, M.; Gill, P. M. W.; Johnson, B.; Chen, W.; Wong, M. W.; Gonzalez, C.; Pople, J. A. *Gaussian 03*, revision C.02; Gaussian, Inc.: Wallingford, CT, 2004.

(32) Sankari, R.; Ehara, M.; Nakatsuji, H.; Senba, Y.; Hosokawa, K.; Yoshida, H.; De, Fanis, A.; Tamenori, Y.; Aksela, S.; Ueda, K. *Chem. Phys. Lett.* **2003**, *380*, 647.

(33) Kirtley, S. M.; Mullins, O. C.; Chen, J.; van Elp, J.; George, S. J.; Chen, C. T.; O'Halloran, T.; Cramer, S. P. *Biochim. Biophys. Acta* **1992**, *1132*, 249.

(34) (a)Fujii, K.; Akamatsu, K.; Muramatsu, Y.; Yokoya, A. *Nucl. Instrum. Methods Phys. Res., Sect. B* **2003**, *199*, 249. (b) Fujii, K.; Akamatsu, K.; Yokoya, A. *J. Phys. Chem. B* **2004**, *108*, 8031.

(35) (a) Hush, N. S.; Cheung, A. S. *Chem. Phys. Lett.* **1975**, *34*, 11. (b) Orlov, V. M.; Smirnov, A. N.; Varshavsky, Y. M. *Tetrahedron Lett.* **1976**, *17*, 4377. (c) Jovanovic, S. V.; Simic, M. G. *J. Phys. Chem.* **1986**, *90*, 974. (d) Colson, A. O.; Besler, B.; Close, D. M.; Sevilla, M. D. *J. Phys. Chem.* **1993**, *97*, 661. (e) Seidel, C. A. M.; Schulz, A.; Sauer, H. M. *J. Phys. Chem.* **1996**, *100*, 5541. (f) Sugiyama, H.; Saito, I. *J. Am. Chem. Soc.* **1996**, *118*, 7063. (g) Steenken, S.; Jovanovic, S. V. *J. Am. Chem. Soc.* **1997**, *119*, 617. (h) Prat, F.; Houk, K. N.; Foote, C. S. *J. Am. Chem. Soc.* **1998**, *120*, 845. (i) Russo, N.; Toscano, M.; Grand, A. *J. Comput. Chem.* **2000**, *21*, 1243.

(36) Ma, Y.; Skytt, P.; Wassdahl, N.; Glans, P.; Mancini, D. C.; Guo, J.; Nordgren, J. *Phys. Rev. Lett.* **1993**, *71*, 3725.

(37) Harada, Y.; Tokushima, T.; Takata, Y.; Takeuchi, T.; Kitajima, Y.; Tanaka, S.; Kayanuma Y.; Shin, S. *Phys. Rev. Lett.* **2004**, *93*, 017401.

(38) Mauri F.; Car, R. *Phys. Rev. Lett.* **1995**, *75*, 3166.

(39) Tanaka, S.; Kayanuma, Y. *Solid State Commun.* **1996**, *100*, 77.